JOURNAL OF MATERIALS SCIENCE 31 (1996) 1903–1907

Interface microstructure and reaction in Gr/Al metal matrix composites

HAINING YANG, MINGYUAN GU, WEIJI JIANG, GUODING ZHANG
State Key Laboratory of MMCs, Shanghai Jiao-Tong University, Shanghai 200030, People's Republic of China

The interface structure in Gr/Al composites fabricated with liquid metal infiltration has been studied using transmission electron microscopy (TEM). Morphologies of interfacial reaction product, aluminium carbide Al_4C_3, formed at different manufacturing parameters were compared and, the growth mechanism of the carbide was studied by means of high resolution electron microscopy (HREM). It has been shown that the morphology of the carbide is intimately related to the processing parameters with which the composites were produced. There are two kinds of interfaces between the carbide and the aluminium matrix. They have different growth mechanisms and relative growth rates under different growth driving forces. Several crystal orientation relationships between the carbide and the aluminium matrix have been observed.

1. Introduction

Aluminium alloy composite materials reinforced with graphite fibre have received broad attention because of their high strength-to-weight ratio and their potential for economical fabrication by liquid metal infiltration of fibre preforms. The mechanical properties of composites are determined comprehensively by the characteristics of matrix, reinforcement and interface, of which the interface was often considered the most crucial parameter. The reaction taking place at the graphite–aluminium interface to form aluminium carbide, Al_4C_3, has long been believed critical in controlling the mechanical properties of Gr/Al composites [1–3]. A moderate interfacial reaction improves the interfacial compatibility and ameliorates the mechanical properties of the composite, whereas an overreaction at the interface has the opposite effect. So, it is very important to understand well the nature of the reaction and, hence, to control the interface reaction in the composites if the full potential of graphite–aluminium as a structural material is to be realized. In the last few years several studies [1–11] have been done on carbon/graphite–aluminium reactions. Khan [10] studied diffusion couples by depositing films of aluminium onto carbon substrates and reported that the carbide grew as single crystals perpendicular to the *c*-axis of the lattice. Other authors [4, 11] performed similar experiments and confirmed that the carbide growth is a diffusion controlled process. However, little published work has described the exact growth patterns of the aluminium carbide in C/Al composites.

In this investigation, the microstructure of the interface and the growth mechanism of the carbide in an Al–0.35 at % Ti alloy composite reinforced with fibres were studied using a number of techniques including TEM, energy dispersive spectroscopy (EDS), selected area diffraction (SAD) and HREM. In addition, the relationship between morphology of aluminium carbide and manufacturing parameters is discussed.

2. Experimental procedure

Two samples, designated A and B, were manufactured using liquid infiltration. Both composites were Al–0.35 at % Ti alloy reinforced with 55 vol % of unidirectional P-55 graphite fibres. The graphite fibre preform was infiltrated at an applied pressure of about 7 MPa. Sample A was cast at a melt temperature of 708 °C and a cooling rate of 8.2 °C min^{-1}. Sample B was prepared at a melt temperature of 748 °C and a cooling rate of 3.7 °C min^{-1}. Ultimate tensile strengths (UTS) of sample A and B are, respectively, 790 and 228 MPa. This very large difference in UTS results mainly from the difference in morphology and amount of interfacial reaction product Al_4C_3, which will be described in detail in the next section.

For the examination in TEM, 3 mm diameter discs were prepared with the longitudinal fibre direction in the plane of the piece. Subsequently, specimens were ground to a thickness of approximately 100 to 120 μm, then mechanically thinned further in a Gatan dimple grinder to a thickness of 5 to 10 μm and finally thinned to perforation in a Gatan ion beam milling apparatus. Thinned specimens were examined in a Philips CM12 transmission electron microscope fitted with a PV9900 EDS.

3. Results

3.1. Interface morphologies

Fig. 1 illustrates interfacial reaction zones of both sample A and sample B composites in which lath-like

0022–2461

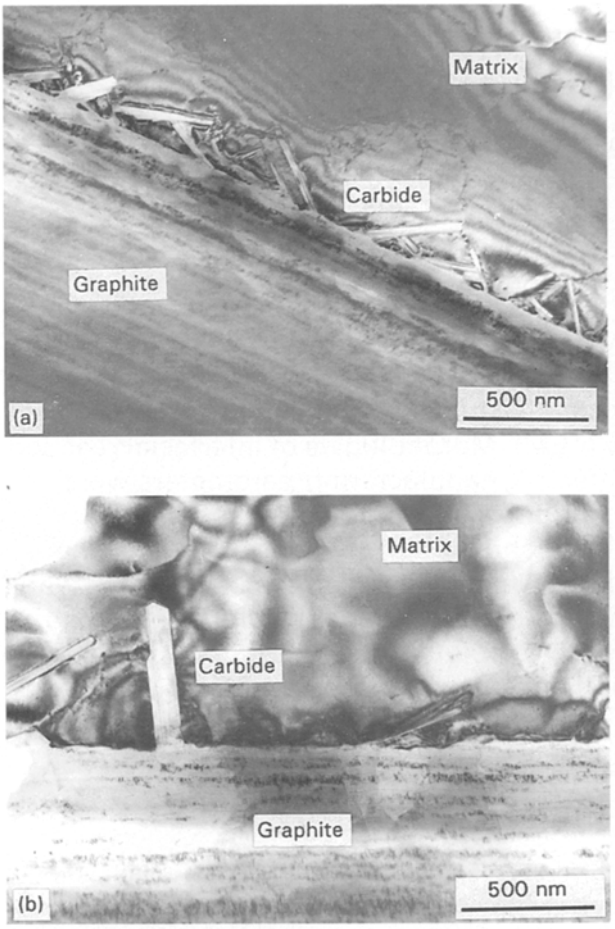

Figure 1 Fibre/matrix interface in Gr/A1–0.35 at %Ti composites. (a) Sample A, cast at a melt temperature of 708 °C and a cooling rate of 8.2 °C per min. (b) Sample B, cast at a melt temperature of 748 °C and a cooling rate of 3.7 °C per min.

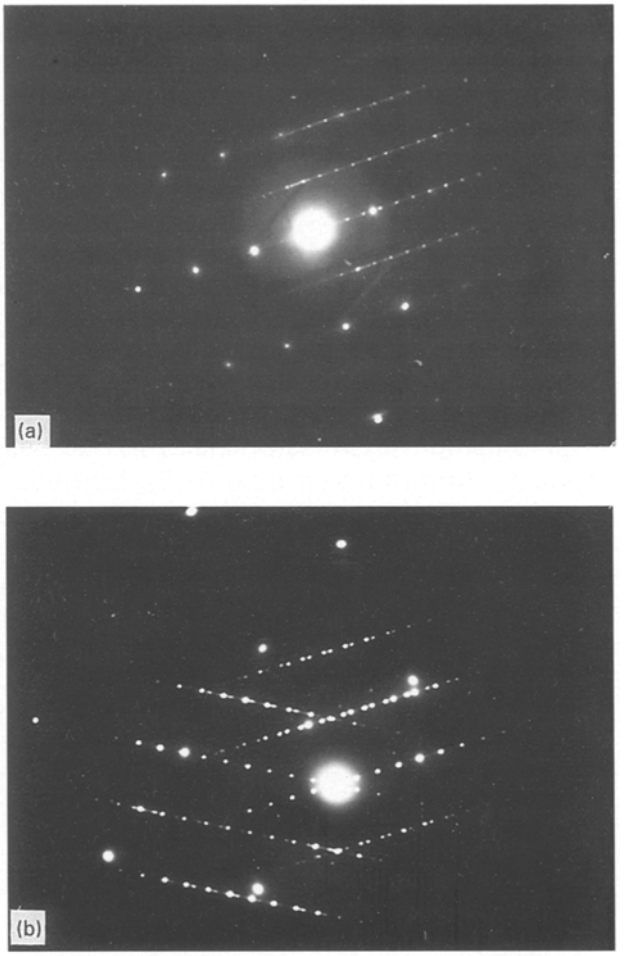

Figure 2 SAD patterns taken from the aluminium/carbide interface regions showing superpositions between carbide and aluminium matrix. (a) with the zone axis of $[\bar{2}\,1\,1]_{Al}//[1\,\bar{2}\,1\,0]_{carbide}$ (b) with the zone axis of $[1\,\bar{1}\,4]_{Al}//[1\,1\,\bar{2}\,0]_{carbide}$. (In addition, a high density of growth twins in the carbide with the $\{0\,0\,0\,1\}$ habit plane are showed.

crystals are shown. The diffraction pattern proves that these crystals are Al_4C_3, which has a hexagonal structure with lattice parameters of $a = 0.33$ nm and $c = 2.49$ nm. It is also proved that the longitudinal axis of the crystal is parallel to the carbide $(0\,0\,0\,1)$ plane and perpendicular to the carbide $[0\,0\,0\,1]$ direction.

Due to different manufacturing parameters, crystals of Al_4C_3 in the interfaces of sample A and B demonstrate different morphologies. Sample A, cast at a lower melt temperature and a more rapid cooling rate, formed small slim crystals of Al_4C_3 with an average length of about 0.35 μm and an aspect ratio of about 10. By contrast, sample B, cast at a higher melt temperature and a slower cooling rate, formed large, broad crystals of Al_4C_3 with an average length of about 0.65 μm and an aspect ratio of about 5. Another feature of the morphology of the carbide is that the large crystals of Al_4C_3 often had growth ledges on their side faces while the small ones often had straight side faces.

3.2. Crystal orientation relationships

In this investigation, several crystal orientation relationships between the carbide and the aluminium matrix have been identified. Two SAD patterns, Fig. 2a and b taken from the aluminium/carbide interface regions, contain diffraction spots from both the aluminium and the carbide. In Fig. 2a, the electron beam direction in the aluminium is $[\bar{2}\,1\,1]$ and in the carbide is $[1\,\bar{2}\,1\,0]$, the interface plane of the carbide crystal is $(0\,0\,0\,1)$, and the aluminium interface plane is $(1\,1\,1)$. This gives the orientation relationship:

$$(0\,0\,0\,1)_{carbide}//(1\,1\,1)_{Al} \text{ with } [1\,\bar{2}\,1\,0]_{carbide}//[\bar{2}\,1\,1]_{Al}$$

Fig. 2b shows the SAD pattern containing spots from the matrix and two carbide crystals, designated as A and B. The zone axis is $[1\,\bar{1}\,4]_{Al}//[\bar{2}\,1\,1\,0]_{carbide\ A}//[1\,1\,\bar{2}\,0]_{carbide\ B}$. The interface planes of the two carbide crystals are $(0\,0\,0\,1)$ and the aluminium interface planes are $(\bar{3}\,1\,1)$ and $(\bar{5}\,\bar{1}\,\bar{1})$, respectively. This gives the orientation relationships:

$$(0\,0\,0\,1)_{carbide}//(\bar{3}\,1\,1)_{Al} \text{ with } [\bar{2}\,1\,1\,0]_{carbide}//[1\,\bar{1}\,4]_{Al}$$

$$(0\,0\,0\,1)_{carbide}//(\bar{5}\,\bar{1}\,1)_{Al} \text{ with } [1\,1\,\bar{2}\,0]_{carbide}//[1\,\bar{1}\,4]_{Al}$$

3.3. Interface between the carbide and the matrix

The results of HREM reveal that the interface between the tip of the lath-like carbide (i.e. the edges of $(0\,0\,0\,1)$ faces) and the Al matrix is an atomically diffuse interface while the interface between the side face of the

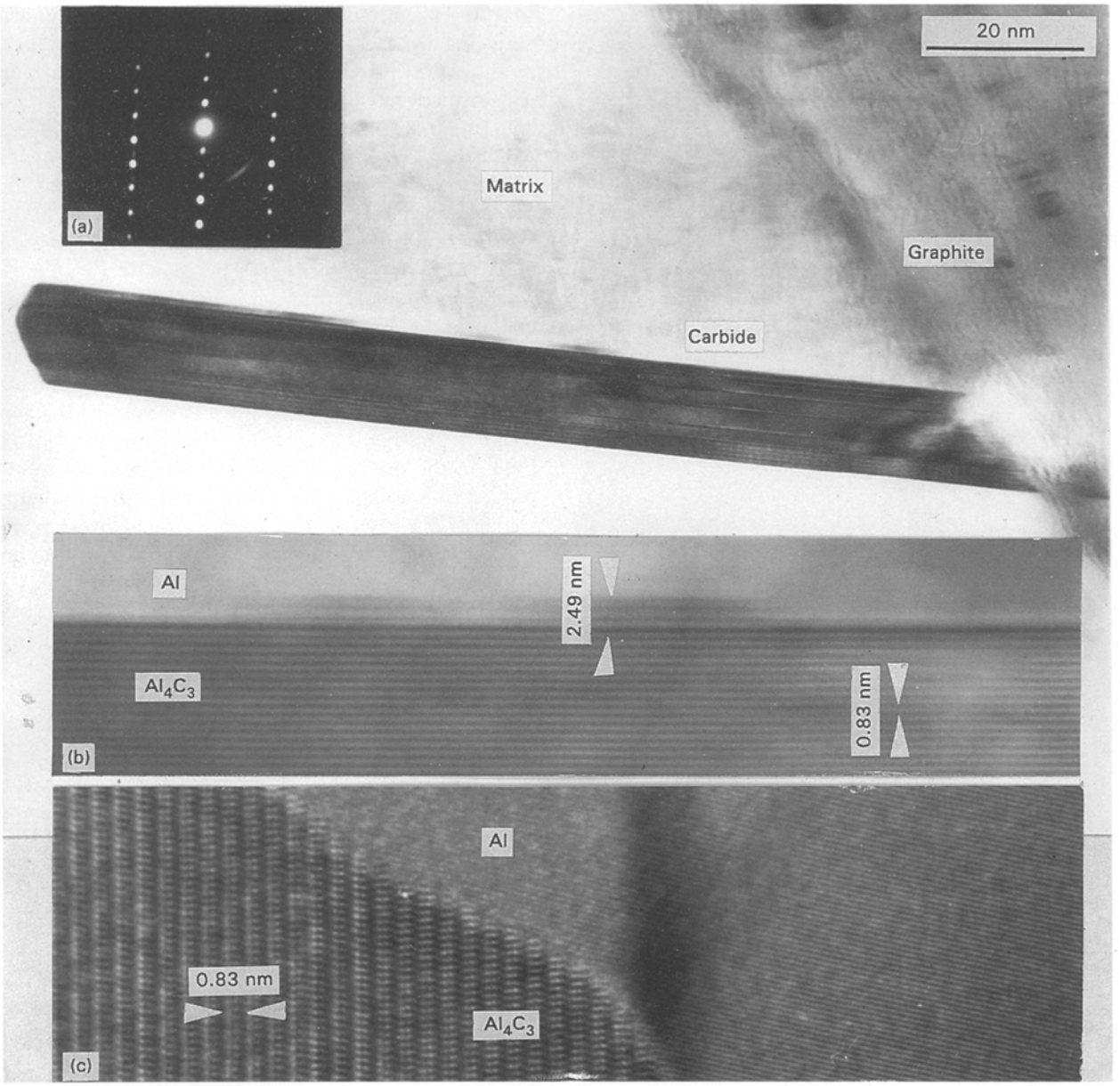

Figure 3 High resolution electron micrograph of Al_4C_3 showing several platelets with a height of 3-fringe spacing on the upper side of the lath-like carbide.

lath-like carbide (i.e. the (0 0 0 1) face) and the Al matrix is a flat interface, as shown in Fig. 3. These two types of interfaces have different growth mechanisms. The diffuse interface migrates in a continuous growth model which is governed by diffusion rates of component atoms. The flat interface grows according to a ledge mechanism which must have occurred by much repeated two-dimensional nucleation or a spiral growth mechanism.

In Fig. 3 several platelets with a height of three fringes are observed along the upper side of the carbide crystal. In this high resolution electron micrograph lattice fringes with a spacing of 0.83 nm lying parallel to the crystal axis are shown. Three fringe spacings correspond to the *c*-axis dimension of Al_4C_3 (2.49 nm).

4. Discussion

Under different growth driving forces, the diffuse interface and the flat interface have different relative growth rates. Generally, under lower growth driving forces, the diffuse interface will migrate much faster than the flat interface. Of the two kinds of flat faces, the face with the spiral growth mechanism grows faster than the face with the two-dimensional nucleation mechanism. As the driving force increases, the flat face will gradually transform to a stepped face [12]. The morphology of a crystal depends on the growth rates of the different crystallographic faces. This explains why sample A manufactured under a lower temperature and a more rapid cooling rate has small carbide crystals with large aspect ratio, and, in contrast, sample B has large carbide crystals with small aspect ratio.

It is noted that the small platelets on the sides of the carbide crystals have typically a three-fringe-spacing thickness, as shown in Fig. 3, which equals the carbide *c*-dimension (2.49 nm). This can be explained on the basis of the crystal structure of the aluminium carbide, which can be described in terms of two structural blocks [13]. These blocks are $[Al_2C_2]_n$ and $[Al_2C]_n$.

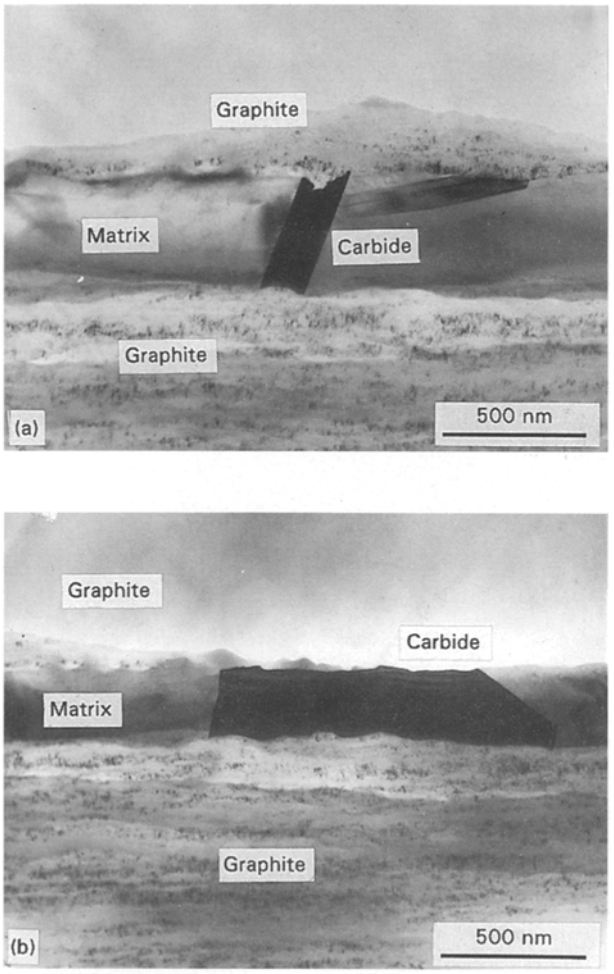

Figure 4 Carbide 'Bridge' (a) and carbide 'Block' (b) formed between two fibres that were closely spaced.

The $[Al_2C_2]_n$ block consists of two adjacent layers of metal atoms with carbon atoms occupying the tetrahedral interstices immediately above and below the double metallic layer. The $[Al_2C]_n$ block consists of two metallic layers with the carbon atoms between them in the six-fold octahedrally coordinated sites. The Al_4C_3 is stacked by three compound blocks with each one consisting of $[Al_2C]_n$ blocks interspersed with $[Al_2C_2]_n$ blocks. Structure of the three compound blocks is the same but there is a 120° rotation around their normal of [0 0 0 1] axis among each other. Because the electron beam is perpendicular to the rotation axis of [0 0 0 1] there will be no difference observed in the one-dimensional HREM microphotograph in Fig. 3 between the three compound blocks. Therefore, the space between each fringe in the microphotograph is one third of the *d*-space of (0 0 0 1) and the three-fringe height equals the lattice constant *c*, i.e. 2.49 nm. It means that only three compound blocks are added to the interface between Al_4C_3 and Al matrix but the coherent relationship between them can be maintained. This structure is stable and often seen in the present investigation.

Fig. 4 shows the morphology of the aluminium carbide in the regions where fibres are closely spaced. In this situation the carbide has two sources of carbon supply. The carbide generated at one Gr/Al interface easily reaches the other interface to become a "bridge", as shown in Fig. 4a. In Fig. 4b a large block carbide was formed between two fibres. It is not difficult to envisage that the carbide between the graphite fibres will become a source of embrittlement resulting in early fracture of the fibres. So, it is advantageous for the improvement of mechanical properties if the fibres are separated uniformly or the volume fraction of fibre is reduced.

The mechanical properties of Gr/Al composites can also be improved through the addition of a small amount of titanium. A significant increase in tensile strength of Gr/Al composites, especially at temperatures between 500–650 °C was achieved when 0.4 at % titanium was added to the aluminium matrix [14]. In the present work, TEM and EDS were employed to investigate the distribution of the titanium element. The results from about 50 sites investigated showed that there was no enrichment of titanium element and no titanium compound at the Gr/Al interface. The titanium is therefore probably improving the mechanical properties by a grain refining action on the aluminium matrix [15].

5. Conclusions

1. There are two kinds of interfaces between the carbide and the aluminium matrix. Under different growth driving forces, they exhibit different relative growth rates resulting in different carbide morphologies.
2. Several crystallographic orientation relationships have been observed between the carbide and aluminium matrix.
3. Neither enrichment of titanium element nor titanium-bearing compounds at the interface was found in this investigation.
4. A carbide "bridge" and "block" were often found between closely spaced fibres.

Acknowledgements

The authors gratefully acknowledge the provision of financial support from National Natural Science Foundation of China. The contract number is 59291005.

References

1. H. NAYEB-HASHEMI and J. SEYYEDI, *Metall. Trans. A* **20A** (1989) 727.
2. M. F. AMATEAN, *J. Compos. Mater.* **10** (1976) 279.
3. A. P. DIWANJI and I. W. HALL, *J. Mater. Sci.* **27** (1992) 2093.
4. S. J. BAKER and W. BONFIELD, *ibid.* **13** (1978) 1329.
5. T. A. CHEMYSHOVA and L. I. KOBELEVA *ibid.* **20** (1985) 3524.
6. W. C. HARRIGAN, Jr., *Metall. Trans. A* **9A** (1978) 503.
7. J. J. MASSON, K. SCHULTE, F. GIROT and Y. LE PETITCORPS, *Mater Sci. Eng.* **A135** (1991) 59.
8. V. D. SCOTT, R. L. TRUMPER and MING YANG, *Compos. Sci. Tech.* **42** (1991) 251.
9. M. YANG and V. D. SCOTT, *J. Mater. Sci.* **26** (1991) 1069.
10. I. H. KHAN, *Metall. Trans.* **7A** (1976) 1281.

11. A. OKURA and H. ASANUMA, *Compos. Sci. Eng.* **24** (1985) 243.
12. MIN NAI-BEN, "Physical Basis of Crystal Growth" (Shanghai Science & Technical Pub., Shanghai, 1983) p. 434 (in Chinese).
13. G. A. JEFFREY and V. Y. WU, *Acta Crystallogr.* **16** (1963) 559.
14. CHEN RONG, Doctoral Dissertation, Shanghai Jiao Tong University (1989) p. 71.
15. L. F. MONDOLFO, "Aluminium Alloys: Structures and Properties" (Butterworth & Co. Ltd., England, 1976) p. 236.

Received 29 June 1994
and accepted 17 July 1995